A HLL_nc (HLL nonconservative) method for the one-dimensional nonconservative Euler system

Stéphane Clain

A HLL_nc (HLL nonconservative) method for the one-dimensional nonconservative Euler system

Stéphane Clain
Institut de mathématiques, CNRS UMR 5219,
Université Paul Sabatier Toulouse 3,
118 route de Narbonne, F-31062 Toulouse cedex 4, France
clain@mip.ups-tlse.fr

Abstract

An adaption of the original HLL scheme for the one-dimensional nonconservative Euler system modeling gaz flow in variational porosity media is proposed . Numerical scheme is detailed and algorithm is tested with two Riemann problems.
Keywords nonconservative Euler system, finite volumes, HLLC.

1 The nonconservative Euler system

We consider the one-dimensional nonconservative Euler system modeling a compressible flow across a porous media:

$$\partial_t \begin{pmatrix} \phi\rho \\ \phi\rho u \\ \phi E \end{pmatrix} + \partial_x \begin{pmatrix} \phi\rho u \\ \phi\rho u^2 + \phi P \\ \phi u(E+P) \end{pmatrix} = \begin{pmatrix} 0 \\ P \\ 0 \end{pmatrix} \partial_x \phi, \tag{1}$$

where ϕ stands for the porosity, ρ the gas density, u the velocity, P the pressure and E the total energy composed of the internal energy e and the kinetic energy: $E = \rho(\frac{1}{2}u^2 + e)$. In addition, we close the system using the perfect gas law $P = (\gamma - 1)\rho e$ with $\gamma > 1$. Such a system casts in the general nonconservative form

$$\partial_t U + \partial_x F(U) = G(U)\partial_x \phi \tag{2}$$

where U stands for the conservative variable vector, $F(U)$ is the conservative flux and $G(U)\partial_x\phi$ represents the nonconservative contribution due to the ϕ parameter derivative.

The conservative quantities (or conservative state) belongs to the conservative variable phase space $\Omega_c \subset \mathbb{R}^+ \times \mathbb{R} \times \mathbb{R}^+$ while the physical (primitive) variables vector $V = (\phi, \rho, u, P)$ belongs to the physical variable phase space $\Omega_p \subset \mathbb{R}^+ \times \mathbb{R}^+ \times \mathbb{R} \times \mathbb{R}^+$. We have a one to one mapping $(\phi, U) \to \widehat{V}(\phi, U)$ such that $V(x,t) = \widehat{V}(\phi(x), U(x,t))$ with inverse function $V \to (\phi, \widehat{U}(V))$ such that $\widehat{U}(V(x,t)) = U(x,t)$. In the sequel, we shall drop the hat symbol for the sake of simplicity and we denote by $F^\alpha(V) = F^\alpha(U(V))$ and $G^\alpha(V) = G^\alpha(U(V))$ with $\alpha = \rho, u, e$ the componants of vector $F(V)$ and $G(V)$ respectively.

2 Steady-state solutions

From a numerical point of view, the main challenge for nonconservative systems is the steady-state preservation of the numerical approximations. Let us consider a regular stationary solution $U(x)$ of system (1), we then have

$$\frac{d}{dx} F(U(x)) = G(U(x)) \frac{d\phi}{dx}. \tag{3}$$

Assume that $\phi = \phi(x)$ is a strictly monotone function on interval $[x^-, x^+]$ with $x^- < 0 < x^+$ which ranges between $\phi^- = \phi(x^-)$, $\phi^+ = \phi(x^+)$ and denote $U^- = U(x^-)$, $U^+ = U(x^+)$. We change the variable x by the variable ϕ setting $U(x) = \widetilde{U}(\phi(x)) = \widetilde{U}(\phi)$ solution of the system

$$\frac{d}{d\phi} F(\widetilde{U}(\phi)) = G(\widetilde{U}(\phi)). \tag{4}$$

We drop the tilde symbol for the sake of simplicity and deduce that $U = U(\phi)$ belongs to an integral curve parameterized with ϕ. For a given U^- and ϕ^-, we have (at least locally) a unique curve $\mathcal{W}(\phi; V^-)$ solution of (4) with $\mathcal{W}(\phi^-; V^-) = U^-$ and $\mathcal{W}(\phi^+; V^-) = U^+$.

The main advantage to use ϕ as a variable is that relation (4) still holds even if $\phi(x)$ is a discontinuous function of x when x^+, x^+ tend to 0. The ability to handle the ϕ discontinuity is of crucial importance for the Riemann problem. Indeed, function ϕ is constant in the open sets $x < 0$ and $x > 0$ and the nonconservative problem turns to a conservative one on each half line as noticed by Andrianov & Warnecke (2004). The nonconservative part only acts at the interface $x = 0$ where ϕ jumps from ϕ^- to ϕ^+.

System (4) provides the three relations

$$(a)\ \phi\rho u = D, \quad (b)\ \frac{d}{d\phi}(\phi\rho u^2 + \phi P) = P, \quad (c)\ u^2 + \frac{2\gamma}{\gamma - 1}\frac{P}{\rho} = H, \tag{5}$$

where D and H are constants which correspond to the mass flow rate and the enthalpy respectively. If $u = 0$, we get that P and ρ are constant. Assuming now that $u \neq 0$ then the curve $\mathcal{W}(\phi, V^-)$ is implicitly given by the three relations (see Clain & Rochette (2009)):

$$\phi\rho u = D, \qquad u^2 + \frac{2\gamma}{\gamma - 1}\frac{P}{\rho} = H, \qquad \frac{P}{\rho^\gamma} = S, \tag{6}$$

where constants D, H and S are determined by the initial condition V^-. We deduce from relation (6) an implicit relation $P = P(\phi)$ given by

$$\frac{D^2}{\phi^2} + \frac{2\gamma}{\gamma - 1} P \left(\frac{P}{S}\right)^{\frac{1}{\gamma}} = H \left(\frac{P}{S}\right)^{\frac{2}{\gamma}}. \tag{7}$$

In particular, when ϕ ranges between ϕ^- and ϕ^+, we deduce from relation (4) the following equality:

$$F^u(U^+) - F^u(U^-) = \int_{\phi^-}^{\phi^+} P(\phi) d\phi. \tag{8}$$

3 The HLL_nc numerical flux

In Toro et al. (1994), the authors propose an extention of the Harten, Lax and Van Leer scheme (Harten et al. (1983)) introducing an intermediate wave which corresponds to the contact discontinuity associated to eigenvalue $\lambda = u$. To evaluate the solution, the authors use the Riemann invariants *i.e.* the pressure and the velocity invariance in the Euler case to provide a new set of equations. Following the same idea, we introduce the intermediate wave which corresponds to the contact discontinuity $\lambda_0 = 0$ deriving from the porosity change across the interface $x = 0$ and use the associated Riemann invariants.

Let us consider the Riemann problem with initial conditions V_L and V_R such that $U(x, 0) = U_L$, $\phi(x) = \phi_L$ for $x < 0$ and $U(x, 0) = U_R$, $\phi(x) = \phi_R$ for $x > 0$. We assume that we know two approximations $S_L < S_R$ of $\lambda_1 = u - c$ and $\lambda_3 = u + c$ respectively and we seek an approximation of the Riemann problem solution introducing intermediate states V_L^*, V_R^* and V_a. Three situations then arise whether $S_R < 0$, $S_L > 0$ or $S_L < 0 < S_R$ (see figure 1). The goal is to evaluate a flux approximation F^- and F^+ on the left and right sides of the interface $x = 0$ which shall be used in the finite volume scheme. We now detail the three situations in the following section.

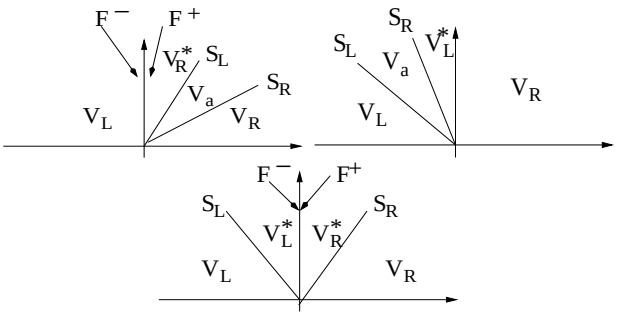

Figure 1: Supersonic configuration with $S_L > 0$ (left), supersonic configuration with $S_R < 0$ (right), subsonic configuration (bottom).

3.1 The supersonic case $S_L > 0$

We first treat the situation when $S_L > 0$. In this case we obtain the following configuration depicted in figure 1 (left). We have to compute $F^- = F_L$ and $F^+ = F_R^*$ to provide the flux accross the interface.

3.1.1 Equations

From the conservation of mass and energy, we have

$$F_L^\rho = F_R^{*,\rho}, \tag{9}$$
$$F_L^P = F_R^{*,P}. \tag{10}$$

On the other hand, we want to preserve the Riemann invariants hence

$$F_L^\rho = \phi_L \rho_L u_L = \phi_R \rho_R^* u_R^*, \tag{11}$$
$$F_L^P = \phi_L u_L (E_L + P_L) = \phi_R u_R^* (E_R^* + P_R^*), \tag{12}$$
$$\frac{P_L}{(\rho_L)^\gamma} = \frac{P_R^*}{(\rho_R^*)^\gamma}. \tag{13}$$

with $E_L = \frac{1}{2}\rho_L (u_L)^2 + \frac{P_L}{\gamma - 1}$ and $E_R^* = \frac{1}{2}\rho_R^* (u_R^*)^2 + \frac{P_R^*}{\gamma - 1}$.

Finally, we use the fact that U_L and U_L^* belong to the same integral curve and relation (8) writes

$$F_R^{*,u} - F_L^u = \int_{\phi_L}^{\phi_R} P(\phi) d\phi = F^u(U_R^*) - F^u(U_L) \tag{14}$$

which leads to $F_R^{*,u} = F^u(U_R^*) = \phi_R(\rho_R^*(u_R^*)^2 + P_R^*)$. Note that the computation of U_a and the other fluxes are not performed since we only require the fluxes on both side of the interface $x = 0$.

To sum-up, we obtain the following system

$$(\mathcal{S}_L) \quad \begin{cases} F_L^{\rho} = \phi_L \rho_L u_L = \phi_R \rho_R^* u_R^* = F_R^{*,\rho}, \\ F_L^{P} = \phi_L u_L (E_L + P_L) = \phi_R u_R^* (E_R^* + P_R^*) = F_R^{*,P}, \\ \frac{P_L}{(\rho_L)^\gamma} = \frac{P_R^*}{(\rho_R^*)^\gamma}, \\ E_L = \frac{1}{2}\rho_L (u_L)^2 + \frac{P_L}{\gamma - 1}, \\ E_R^* = \frac{1}{2}\rho_R^* (u_R^*)^2 + \frac{P_R^*}{\gamma - 1}, \\ F_R^{*,u} = \phi_R (\rho_R^* (u_R^*)^2 + P_R^*), \end{cases}$$

where ϕ_L, ρ_L, u_L, P_L, ϕ_R are given and ρ_R^*, u_R^*, P_R^*, F_R^* are the unknowns.

3.1.2 Resolution

To solve system $(\mathcal{S}_L)$, we introduce a function

$$\rho \to g_{sup}(\rho; V_L, \phi_R) = g_{sup}(\rho)$$

such that $g_{sup}(\rho_R^*) = 0$. For a given predicted value ρ_R^*, we compute P_R^* with relation (13)

$$P_R^* = P_R^*(\rho_R^*) = P_L \frac{(\rho_R^*)^\gamma}{(\rho_L)^\gamma}.$$

Using relation (11), we deduce the velocity

$$u_R^* = u_R^*(\rho_R^*) = u_L \frac{\phi_L \rho_L}{\phi_R \rho_R^*}.$$

On the other hand, relations (12) and (11) give

$$\frac{E_L + P_L}{\rho_L} = \frac{E_R^* + P_R^*}{\rho_R^*}$$

which provides the equality

$$E_R^* = E_R^*(\rho_R^*) = (E_L + P_L)\frac{\rho_R^*}{\rho_L} - P_R^*.$$

Let us define the function

$$g_{sup}(\rho_R^*) = E_R^* - \frac{1}{2}\rho_R^* (u_R^*)^2 - \frac{P_R^*}{\gamma - 1},$$

we then seek ρ_R^* such that $g_{sup}(\rho_R^*) = 0$ where the physical state $V_R^* = (\phi_R, \rho_R^*, u_R^*, P_R^*)$ has to correspond to a supersonic state.

Problem $(\mathcal{S}_L)$ has zero, one or two solutions (see Clain & Rochette (2009)). For the two zeros cases, we have $\rho_{sup} < \rho_{sub}$ and choose ρ_{sup} which corresponds to the supersonic case. Numericaly, we employ a Lagrange algorithm or an inexact Newton method taking a very small value for ρ as an initial condition to converge to density ρ_{sup}.

3.2 The supersonic case $S_R < 0$

In case $S_R < 0$, we have to compute $F^- = F_L^*$ and $F^+ = F_R$ to provide the flux accross the interface. The system of equation is similar to the previous one where we substitute variables V_L and V_R^* with V_L^* and V_R respectively.

3.3 The subsonic case

We now face the more complex situation since all the states have to be estimated to compute $F^- = F_L^*$ and $F^+ = F_R^*$. We consider the configuration depicted in figure (1, bottom) where we assume that V_L and V_L^* are separated with a shock of velocity S_L and V_R and V_R^* by a shock of velocity S_R while interface $x = 0$ corresponds to the porosity change.

3.3.1 Equations

Rankine-Hugoniot relations associated to the waves S_L and S_R yield

$$\begin{aligned} F_L^* - F_L &= S_L(U_L^* - U_L), & (15)\\ F_R^* - F_R &= S_R(U_R^* - U_R). & (16) \end{aligned}$$

On the other hand, we assume that V_L^* and V_R^* are linked with the Riemann invariants across the contact discontinuity generated by the porosity hence

$$\begin{aligned} \phi_R \rho_R^* u_R^* &= \phi_L \rho_L^* u_L^*, & (17)\\ \phi_R u_R^*(E_R^* + P_R^*) &= \phi_L u_L^*(E_L^* + P_L^*), & (18)\\ \frac{P_R^*}{(\rho_R^*)^\gamma} &= \frac{P_L^*}{(\rho_L^*)^\gamma}. & (19) \end{aligned}$$

For the density and the energy equations, relations cast in the conservative form

$$\begin{aligned} F_R^{*,\rho} &= F_L^{*,\rho}, & (20)\\ F_R^{*,P} &= F_L^{*,P}. & (21) \end{aligned}$$

For the impulsion equation, since U_L^* and U_R^* belongs to the same integral curve, the flux variation across the interface is given by

$$F_R^{*,u} - F_L^{*,u} = \int_{\phi_L}^{\phi_R} P(\phi) d\phi = F^u(U_R^*) - F^u(U_L^*). \quad (22)$$

At last, the definition of the total energy gives

$$E_\alpha^* = \frac{1}{2}\rho_\alpha^*(u_\alpha^*)^2 + \frac{P_\alpha^*}{\gamma - 1}, \quad \alpha = L, R. \quad (23)$$

To sum-up, we obtain the following system ($\mathcal{S}_{sub}$)

$$\begin{aligned}
\phi_R\rho_R^*u_R^* &= \phi_L\rho_L^*u_L^*, && (24)\\
\frac{P_R^*}{(\rho_R^*)^\gamma} &= \frac{P_L^*}{(\rho_L^*)^\gamma}, && (25)\\
\phi_R u_R^*(E_R^*+P_R^*) &= \phi_L u_L^*(E_L^*+P_L^*), && (26)\\
F_R^\rho - S_R\phi_R\rho_R + S_R\phi_R\rho_R^* &= F_L^\rho - S_L\phi_L\rho_L + S_L\phi_L\rho_L^*, && (27)\\
F_R^P - S_R\phi_R E_R + S_R\phi_R E_R^* &= F_L^P - S_L\phi_L E_L + S_L\phi_L E_L^*, && (28)\\
F_R^{*,u} - \phi_R(\rho_R^*(u_R^*)^2 + P_R^*) &= F_L^{*,u} - \phi_L(\rho_L^*(u_L^*)^2 + P_L^*) && (29)\\
F_L^{*,u} &= F_L^u + S_L\phi_L(\rho_L^*u_L^* - \rho_L u_L), && (30)\\
F_R^{*,u} &= F_R^u + S_R\phi_R(\rho_R^*u_R^* - \rho_R u_R) && (31)\\
E_L^* &= \frac{1}{2}\rho_L^*(u_L^*)^2 + \frac{P_L^*}{\gamma-1} && (32)\\
E_R^* &= \frac{1}{2}\rho_R^*(u_R^*)^2 + \frac{P_R^*}{\gamma-1}, && (33)
\end{aligned}$$

3.3.2 Resolution

To solve system (24)-(33), we introduce a function $\rho \to g_{sub}(\rho)$ such that $g_{sub}(\rho_L^*) = 0$. For a given predicted value ρ_L^*, we compute

$$\rho_R^* = \rho_R^*(\rho_L^*) = \frac{1}{S_R\phi_R}(F_L^\rho - F_R^\rho - S_L\phi_L\rho_L + S_R\phi_R\rho_R + S_L\phi_L\rho_L^*).$$

and relations (26) and (24) yield

$$\frac{E_R^*+P_R^*}{\rho_R^*} = \frac{E_L^*+P_L^*}{\rho_L^*}, \tag{34}$$

while relations (32), (33) and (24) give

$$\phi_L^2\rho_L^*\left(E_L^* - \frac{P_L^*}{\gamma-1}\right) = \phi_R^2\rho_R^*\left(E_R^* - \frac{P_R^*}{\gamma-1}\right). \tag{35}$$

Relations (25), (28), (34) and (35) give the following linear system

$$(\mathcal{LS})\begin{pmatrix} \frac{1}{(\rho_L^*)^\gamma} & -\frac{1}{(\rho_R^*)^\gamma} & 0 & 0\\ \frac{1}{\rho_L^*} & -\frac{1}{\rho_R^*} & \frac{1}{\rho_L^*} & -\frac{1}{\rho_R^*}\\ -\phi_L^2\frac{\rho_L^*}{\gamma-1} & \phi_R^2\frac{\rho_R^*}{\gamma-1} & \phi_L^2\rho_L^* & -\phi_R^2\rho_R^*\\ 0 & 0 & \phi_L S_L & -\phi_R S_R \end{pmatrix}\begin{pmatrix} P_L^*\\ P_R^*\\ E_L^*\\ E_R^* \end{pmatrix} = \begin{pmatrix} 0\\ 0\\ 0\\ \kappa \end{pmatrix}$$

with

$$\kappa = F_R^P - F_L^P + S_L\phi_L E_L - S_R\phi_R E_R.$$

and we deduce $P_L^*(\rho_L^*)$, $P_R^*(\rho_L^*)$, $E_R^*(\rho_L^*)$ and $E_L^*(\rho_L^*)$.

Substituting $F_L^{*,u}$ from equation (30) and $F_R^{*,u}$ from equation (31) in relation (29) provide

$$\begin{aligned} F_R^u + S_R\phi_R(\rho_R^* u_R^* - \rho_R u_R) - 2\phi_R E_R^* + \phi_R \tfrac{3-\gamma}{\gamma-1} P_R^* &= \\ F_L^u + S_L\phi_L(\rho_L^* u_L^* - \rho_L u_L) - 2\phi_L E_L^* + \phi_L \tfrac{3-\gamma}{\gamma-1} P_L^*. & \end{aligned} \tag{36}$$

Mass flow $D = \phi_R\rho_R^* u_R^* = \phi_L\rho_L^* u_L^*$ is then given by

$$\begin{aligned} D(\rho_L^*) &= \frac{1}{S_R - S_L}\Big(\Big[F_L^u - S_L\phi_L\rho_L u_L - 2\phi_L E_L^* + \phi_L\frac{3-\gamma}{\gamma-1}P_L^*\Big] - \\ &\qquad \Big[F_R^u - S_R\phi_R\rho_R u_R - 2\phi_R E_R^* + \phi_R\frac{3-\gamma}{\gamma-1}P_R^*\Big]\Big) \end{aligned}$$

and we finally compute u_L^*, u_R^* with relation (24). The predicted value ρ_L^* if a correct estimate is relation (32) or (33) are satisfied so we define

$$g_{sub}(\rho_L^*) = E_L^*(\rho_L^*) - \frac{1}{2}\rho_L^*(u_L^*)^2 - \frac{P_L^*}{\gamma-1}. \tag{37}$$

4 Numerical tests

Two Riemann problems are considered to test the new scheme. The following table gives the initial conditions where the initial discontinuity is situated at $x = 0.8$. We use uniform mesh of 200 cells on domain $[0, 2]$ while the time step is controled by the classical CFL condition.

	ϕ	ρ $(kg.m^{-3})$	u $(m.s^{-1})$	P (Pa)
V_L (supersonic case)	0.9	1.00	500	50000
V_R (supersonic case)	1.0	3.26	342	75000
V_L (subsonic case)	1.0	3.6	100	300000
V_R (subsonic case)	0.9	3.24	154	200000

We plot in figure (2) the density, pressure and velocity of two approximations (see Clain & Rochette (2009) for the Rusanov nonconservative scheme) and exact solution for the supersonic situation. We observe that the 0-contact discontinuity is very well approximated due to the specific scheme we employ. Figure (2, right bottom) represents function g_{sup} where the smaller zero corresponds to ρ_R^*. Note that the Lagrange algorithm easily converges since the bassin convergence is very large.

We plot in figure (3) the density, pressure and velocity of two approximations and exact solution for the subsonic situation. We observe that

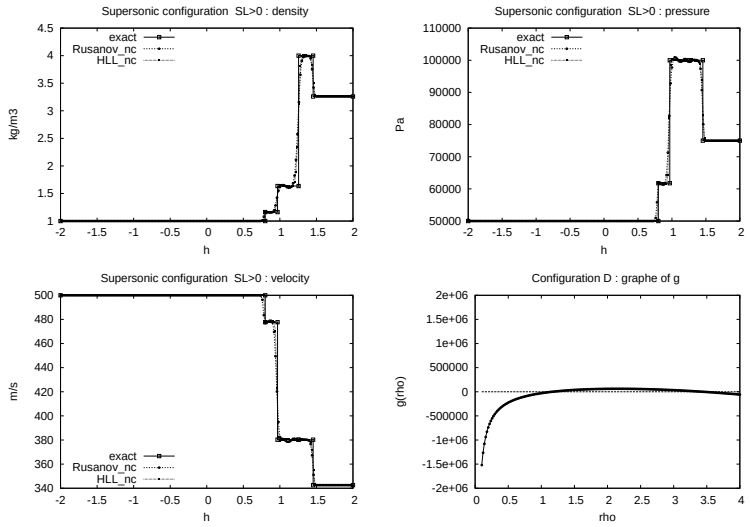

Figure 2: Supersonic configuration. Comparison between the approximated and the exact solution.

the 0-contact discontinuity is still very well approximated while the other shock waves are smooth due to the numerical viscosity. Figure (3, right bottom) represent function g_{sub}. We have two branches but only the left one has a physical interest. The bassin convergence is narrow and Lagrange algorithm fails if one starts with a wrong predicted density (on the wrong branch for example).

References

N. Andrianov and G. Warnecke, On the solution to the Riemann problem for the compressible duct flow, SIAM J. Appl. Math. Vol. 64, No 3 (2004) 878–901.

S. Clain, D. Rochette, First- and Second-order finite volume methods for the one-dimensional nonconservative Euler system, J. Comp. Physics Vol. 228 (2009) 8214-8248.

A. Harten, P. D. Lax, B. van Leer, On upstream differencing and Godunov-type schemes for hyperbolic conservation laws, SIAM review Vol. 25, (1983) 35–61.

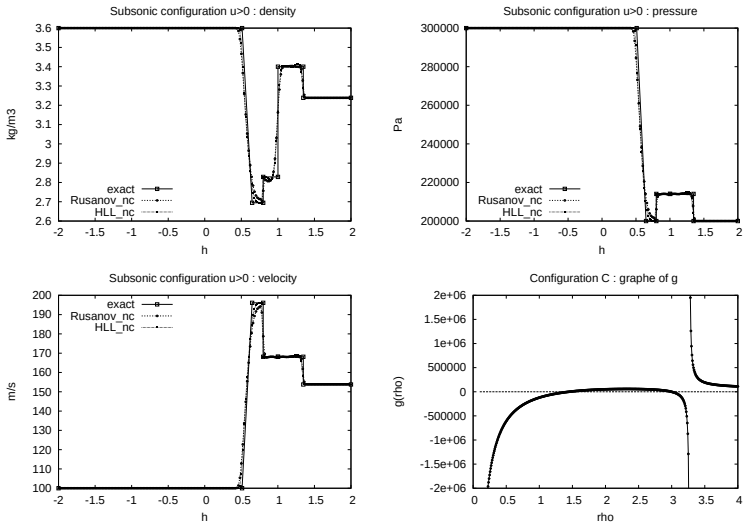

Figure 3: Subsonic configuration. Comparison between the approximated and the exact solution.

E. F. Toro, M. Spruce, W. Speares, Restoration of the contact surface in the HLL-Riemann solver, Shock Waves Vol. 4, (1994) 25–34.